International Conference on Mathematics, Computational Methods & Reactor Physics (M&C 2009)
Saratoga Springs, New York, May 3-7, 2009, on CD-ROM, American Nuclear Society, LaGrange Park, IL (2009)

A QUASI-STATIC CLOSURE FOR 3RD ORDER SPHERICAL HARMONICS TIME-DEPENDENT RADIATION TRANSPORT IN 2-D

Kyeong Sam Oh and James Paul Holloway
Department of Nuclear Engineering and Radiological Sciences,
Collage of Engineering, University of Michigan
2355 Bonisteel, Ann Arbor, MI 48109-2014, USA
ohks@umich.edu; hagar@umich.edu

ABSTRACT

The spherical harmonics (P_N) method is widely used in solving the radiation transport problem, but none of the P_N results is a good approximation to the transport solution at early times for a pulsed source problem since the solution for the scalar flux will show negative oscillations. In an earlier paper [3] McClarren and Holloway suggested a modification for the P_N method by applying a quasi-static approximation to the 3rd order time-dependent current terms. In this paper that modification is tested. The numerical results demonstrate the modified P_N results are less negative at early times and closer to the transport solution at late times than the conventional P_N results.

Key Words: Time-dependent transport; Spherical harmonics; Quasi-static closure; negative flux

1. INTRODUCTION

The time-dependent transport equation has previously been solved in 2-D using spherical harmonic expansions [1, 2, 3]. One interesting result of this work was the realization that the scalar flux in the time-dependent spherical harmonics equations in 2 and 3-D can become negative. This has recently [4] been proven to be the result of a model that is linear, hyperbolic, rotationally invariant, and has finite angular resolution. There is therefore some interest in relaxing each of these conditions to see if a model can be developed for time-dependent transport based on low order angular information that retains some of these physical properties and yet maintains a positive scalar flux. Linearity has been relaxed in the Minerbo closure (see [5]), and rotational invariance has been eliminated in the discrete ordinates method [6] and then both maintain a positive scalar flux. This leaves relaxation of hyperbolicity. In [3] McClarren and Holloway suggested that a quasi-static approximation to the highest order spherical harmonics equation might be a route to this. Such a quasi-static approximation is made in P_1 theory (time-derivative of the current is dropped) to derive time-dependent diffusion theory, and this approximation maintains a positive flux. The simplified P_N method does not provide a positive scalar flux even in 1-D, but a quasi-static approximation to it does [7]. In this paper we will explore such a quasi-static closure in P_3 in 2-D to see if a negative flux can result. We will show numerically that the scalar flux can still go negative in a pulsed source problem in 2-D, and so conclude that this approximation is still not robust.

2. P_3 EQUATIONS FOR TIME-DEPENDENT NEUTRON TRANSPORT

The one-speed time-dependent neutron transport equation can be written as [8]

$$\frac{1}{v}\frac{\partial}{\partial t}\psi(r,\Omega,t) + \Omega\cdot\nabla\psi(r,\Omega,t) + \Sigma_t\psi(r,\Omega,t) = \int_{4\pi}\frac{\Sigma_s}{4\pi}\psi(r,\Omega,t)\,d\Omega + S(r,\Omega,t) \quad (1)$$

where ψ is the angular flux, v is a neutron speed, Ω is the angular variable, Σ_t, Σ_s are the total and scattering cross section respectively, and S is an independent or external source. The cross sections are assumed constant in space and time. The P_N method for the neutron transport equation writes the angular dependence of Eq. (1) as a series expansion in spherical harmonics Y_l^m, and in 2D this results [1] in the system of equations

$$\frac{\partial}{\partial t}\psi_0^0 - \sqrt{\frac{2}{3}}\frac{\partial}{\partial x}\psi_1^1 + \sqrt{\frac{1}{3}}\frac{\partial}{\partial z}\psi_1^0 + \Sigma_t\psi_0^0 = \Sigma_s\psi_0^0 \quad (2)$$

$$\frac{\partial}{\partial t}\psi_1^0 - \sqrt{\frac{2}{5}}\frac{\partial}{\partial x}\psi_2^1 + \sqrt{\frac{1}{3}}\frac{\partial}{\partial z}\psi_0^0 + \sqrt{\frac{4}{15}}\frac{\partial}{\partial z}\psi_2^0 + \Sigma_t\psi_1^0 = 0 \quad (3)$$

$$\frac{\partial}{\partial t}\psi_2^0 + \sqrt{\frac{2}{15}}\frac{\partial}{\partial x}\psi_1^1 - \sqrt{\frac{12}{35}}\frac{\partial}{\partial x}\psi_3^1 + \sqrt{\frac{4}{15}}\frac{\partial}{\partial z}\psi_1^0 + \sqrt{\frac{9}{35}}\frac{\partial}{\partial z}\psi_3^0 + \Sigma_t\psi_2^0 = 0 \quad (4)$$

$$\frac{\partial}{\partial t}\psi_3^0 + \sqrt{\frac{6}{35}}\frac{\partial}{\partial x}\psi_2^1 + \sqrt{\frac{9}{35}}\frac{\partial}{\partial z}\psi_2^0 + \Sigma_t\psi_3^0 = 0 \quad (5)$$

$$\frac{\partial}{\partial t}\psi_1^1 - \sqrt{\frac{1}{6}}\frac{\partial}{\partial x}\psi_0^0 + \sqrt{\frac{1}{30}}\frac{\partial}{\partial x}\psi_2^0 - \sqrt{\frac{1}{5}}\frac{\partial}{\partial x}\psi_2^2 + \sqrt{\frac{1}{5}}\frac{\partial}{\partial z}\psi_2^1 + \Sigma_t\psi_1^1 = 0 \quad (6)$$

$$\frac{\partial}{\partial t}\psi_2^1 - \sqrt{\frac{1}{10}}\frac{\partial}{\partial x}\psi_1^0 + \sqrt{\frac{3}{70}}\frac{\partial}{\partial x}\psi_3^0 - \sqrt{\frac{1}{7}}\frac{\partial}{\partial x}\psi_3^2 + \sqrt{\frac{1}{5}}\frac{\partial}{\partial z}\psi_1^1 + \sqrt{\frac{8}{35}}\frac{\partial}{\partial z}\psi_3^1 + \Sigma_t\psi_2^1 = 0 \quad (7)$$

$$\frac{\partial}{\partial t}\psi_3^1 - \sqrt{\frac{3}{35}}\frac{\partial}{\partial x}\psi_2^0 + \sqrt{\frac{1}{70}}\frac{\partial}{\partial x}\psi_2^2 + \sqrt{\frac{8}{35}}\frac{\partial}{\partial z}\psi_2^1 + \Sigma_t\psi_3^1 = 0 \quad (8)$$

$$\frac{\partial}{\partial t}\psi_2^2 - \sqrt{\frac{1}{5}}\frac{\partial}{\partial x}\psi_1^1 + \sqrt{\frac{1}{70}}\frac{\partial}{\partial x}\psi_3^1 - \sqrt{\frac{3}{14}}\frac{\partial}{\partial x}\psi_3^3 + \sqrt{\frac{1}{7}}\frac{\partial}{\partial z}\psi_3^2 + \Sigma_t\psi_2^2 = 0 \quad (9)$$

$$\frac{\partial}{\partial t}\psi_3^2 - \sqrt{\frac{1}{7}}\frac{\partial}{\partial x}\psi_1^1 + \sqrt{\frac{1}{7}}\frac{\partial}{\partial z}\psi_2^2 + \Sigma_t\psi_3^2 = 0 \quad (10)$$

$$\frac{\partial}{\partial t}\psi_3^3 - \sqrt{\frac{3}{14}}\frac{\partial}{\partial x}\psi_2^2 + \Sigma_t\psi_3^3 = 0\,. \quad (11)$$

3. QUASI-STATIC CLOSURE

In diffusion theory the time-rate-of-change of the current (first order expansion coefficients) is set to zero; in a P_3 approximation we can instead make the quasi-static approximation at the 3rd order coefficients, namely $\frac{\partial}{\partial t}\psi_3^m \approx 0$ and so Eqs. (5), (8), (10) and (11) then allow us to eliminate the 3rd order coefficients as

$$\psi_3^0 = -\frac{1}{\Sigma_t}\left(\sqrt{\frac{6}{35}}\frac{\partial}{\partial x}\psi_2^1 + \sqrt{\frac{9}{35}}\frac{\partial}{\partial z}\psi_2^0\right) \tag{12}$$

$$\psi_3^1 = -\frac{1}{\Sigma_t}\left(-\sqrt{\frac{3}{35}}\frac{\partial}{\partial x}\psi_2^0 + \sqrt{\frac{1}{70}}\frac{\partial}{\partial x}\psi_2^2 + \sqrt{\frac{8}{35}}\frac{\partial}{\partial z}\psi_2^1\right) \tag{13}$$

$$\psi_3^2 = -\frac{1}{\Sigma_t}\left(-\sqrt{\frac{1}{7}}\frac{\partial}{\partial x}\psi_2^1 + \sqrt{\frac{1}{7}}\frac{\partial}{\partial z}\psi_2^2\right) \tag{14}$$

$$\psi_3^3 = -\frac{1}{\Sigma_t}\left(-\sqrt{\frac{3}{14}}\frac{\partial}{\partial x}\psi_2^2\right). \tag{15}$$

Substituting Eq. (12) - (15) into the remaining 6 equations Eq. (2) - (11) gives a new model, which we call the P_3 with quasi-static closure.

$$\frac{\partial}{\partial t}\psi_0^0 - \sqrt{\frac{2}{3}}\frac{\partial}{\partial x}\psi_1^1 + \sqrt{\frac{1}{3}}\frac{\partial}{\partial z}\psi_1^0 + \Sigma_t\psi_0^0 = \Sigma_s\psi_0^0 \tag{16}$$

$$\frac{\partial}{\partial t}\psi_1^0 - \sqrt{\frac{2}{5}}\frac{\partial}{\partial x}\psi_2^1 + \sqrt{\frac{1}{3}}\frac{\partial}{\partial z}\psi_0^0 + \sqrt{\frac{4}{15}}\frac{\partial}{\partial z}\psi_2^0 + \Sigma_t\psi_1^0 = 0 \tag{17}$$

$$\frac{\partial}{\partial t}\psi_2^0 + \sqrt{\frac{2}{15}}\frac{\partial}{\partial x}\psi_1^1 + \sqrt{\frac{4}{15}}\frac{\partial}{\partial z}\psi_1^0 - \frac{1}{\Sigma_t}\frac{6}{35}\frac{\partial^2}{\partial x^2}\psi_2^0 + \frac{1}{\Sigma_t}\frac{2\sqrt{6}}{70}\frac{\partial^2}{\partial x^2}\psi_2^2 - \frac{1}{\Sigma_t}\frac{9}{35}\frac{\partial^2}{\partial z^2}\psi_2^0 + \frac{1}{\Sigma_t}\frac{\sqrt{6}}{35}\frac{\partial^2}{\partial x\partial z}\psi_2^1 + \Sigma_t\psi_2^0 = 0 \tag{18}$$

$$\frac{\partial}{\partial t}\psi_1^1 - \sqrt{\frac{1}{6}}\frac{\partial}{\partial x}\psi_0^0 + \sqrt{\frac{1}{30}}\frac{\partial}{\partial x}\psi_2^0 - \sqrt{\frac{1}{5}}\frac{\partial}{\partial x}\psi_2^2 + \sqrt{\frac{1}{5}}\frac{\partial}{\partial z}\psi_2^1 + \Sigma_t\psi_1^1 = 0 \tag{19}$$

$$\frac{\partial}{\partial t}\psi_2^1 - \sqrt{\frac{1}{10}}\frac{\partial}{\partial x}\psi_1^0 + \sqrt{\frac{1}{5}}\frac{\partial}{\partial z}\psi_1^1 - \frac{1}{\Sigma_t}\frac{8}{35}\frac{\partial^2}{\partial x^2}\psi_2^1 - \frac{1}{\Sigma_t}\frac{8}{35}\frac{\partial^2}{\partial z^2}\psi_2^1 + \frac{1}{\Sigma_t}\frac{\sqrt{6}}{70}\frac{\partial^2}{\partial x\partial z}\psi_2^0 + \frac{1}{\Sigma_t}\frac{3}{35}\frac{\partial^2}{\partial x\partial z}\psi_2^2 + \Sigma_t\psi_2^1 = 0 \tag{20}$$

$$\frac{\partial}{\partial t}\psi_2^2 - \sqrt{\frac{1}{5}}\frac{\partial}{\partial x}\psi_1^1 + \frac{1}{\Sigma_t}\frac{\sqrt{6}}{70}\frac{\partial^2}{\partial x^2}\psi_2^0 - \frac{1}{\Sigma_t}\frac{8}{35}\frac{\partial^2}{\partial x^2}\psi_2^2 - \frac{1}{\Sigma_t}\frac{1}{7}\frac{\partial^2}{\partial z^2}\psi_2^2 + \frac{1}{\Sigma_t}\frac{3}{35}\frac{\partial^2}{\partial x\partial z}\psi_2^1 + \Sigma_t\psi_2^2 = 0. \tag{21}$$

Note that these equations now contain second order derivative terms, like time-dependent diffusion theory. The 1-D form of P_3 with a quasi-static closure can be obtained from Eq. (16) - (18) by dropping x-dependent terms as,

$$\frac{\partial}{\partial t}\psi_0^0 + \sqrt{\frac{1}{3}}\frac{\partial}{\partial z}\psi_1^0 + \Sigma_t\psi_0^0 = \Sigma_s\psi_0^0 \tag{22}$$

$$\frac{\partial}{\partial t}\psi_1^0 + \sqrt{\frac{1}{3}}\frac{\partial}{\partial z}\psi_0^0 + \sqrt{\frac{4}{15}}\frac{\partial}{\partial z}\psi_2^0 + \Sigma_t\psi_1^0 = 0 \tag{23}$$

$$\frac{\partial}{\partial t}\psi_2^0 + \sqrt{\frac{4}{15}}\frac{\partial}{\partial z}\psi_1^0 - \frac{1}{\Sigma_t}\frac{9}{35}\frac{\partial^2}{\partial z^2}\psi_2^0 + \Sigma_t\psi_2^0 = 0 \quad . \tag{24}$$

4. THE DISCRETIZATION METHOD TO SOLVE THE EQUATION

The 2-D P_3 with quasi-static closure consists of six-coupled partial differential equations. We can rewrite Eq. (16) - (21) in a generalized form la.

$$\frac{\partial}{\partial t}u + A_x\frac{\partial}{\partial x}u + A_z\frac{\partial}{\partial z}u + B_x\frac{\partial^2}{\partial x^2}u + B_z\frac{\partial^2}{\partial z^2}u + D\frac{\partial^2}{\partial x\partial z}u + Eu = 0 \tag{25}$$

where $u(x,z,t) = \left[u_0 \quad u_1 \quad u_2 \quad u_3 \quad u_4 \quad u_5\right]^T = \left[\psi_0^0 \quad \psi_1^0 \quad \psi_2^0 \quad \psi_1^1 \quad \psi_2^1 \quad \psi_2^2\right]^T$ and A_x, A_z are the Jacobians of the first order advection terms and then B_x, B_z, D and E are constant matrices. For simplification, we set $C = B_x\frac{\partial^2}{\partial x^2}u + B_z\frac{\partial^2}{\partial z^2}u + D\frac{\partial^2}{\partial x\partial z}u + Eu$ in Eq. (25) to obtain,

$$\frac{\partial}{\partial t}u + A_x\frac{\partial}{\partial x}u + A_z\frac{\partial}{\partial z}u + C = 0 \ . \tag{26}$$

This is a hyperbolic equation with source C containing the second order derivatives. We solve this with a high resolution Riemann solver using a harmonic mean limiter [9], with the second derivatives in C centrally differenced. An explicit forward Euler time-differencing is used. The resulting method is called P_3QS .

5. NUMERICAL RESULTS

5.1. One-dimensional problem

The one-dimensional time-dependent behavior is tested by solving for the scalar flux in a slab. The slab size is 4 cm and consists of a purely scattering medium ($\Sigma_t = \Sigma_s = 1\ \text{cm}^{-1}$). A delta function initially isotropic flux is imposed. The spatial grid and time steps initially are chosen as $\Delta x = 0.002$, $\Delta t = 0.001$ respectively.

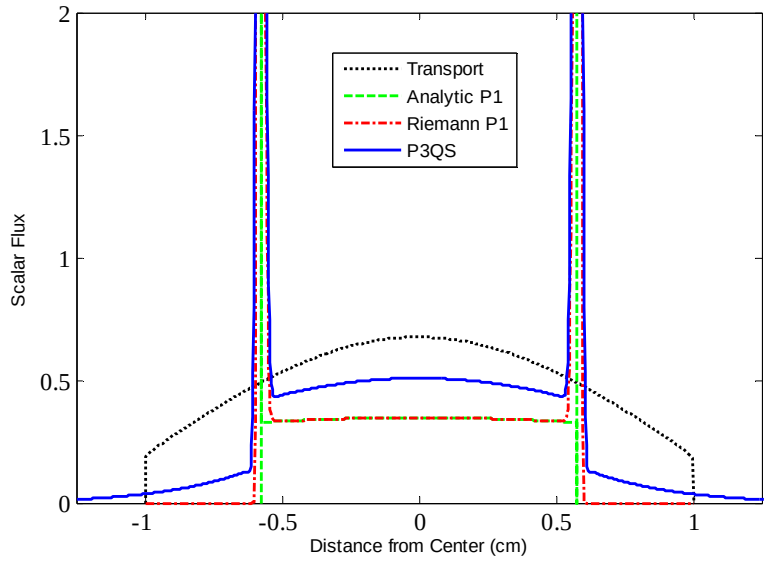

Figure 1. Comparison of P_3QS solution with P_1 and the transport solution at 1 second after the pulse

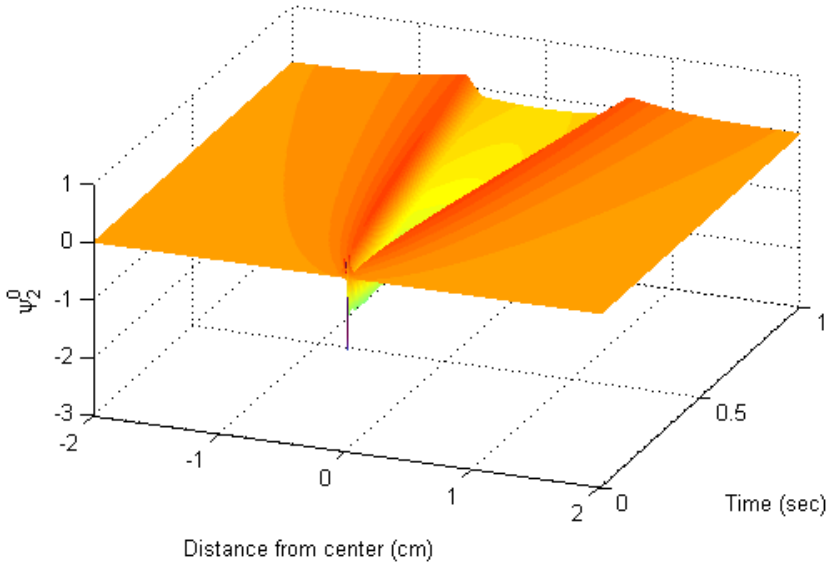

Figure 2. ψ_2^0 of P_3QS solution as a function of time and space

Figure 1 shows comparison of P_1, transport and P_3QS solution at one second after the pulse. The transport result is from the Ganapol's analytic solution [10, 11]. The collided flux shown between the two wave fronts in P_3QS agrees better with the transport solution than does P_1. Note the positive flux in front of the two wave fronts of P_3QS; this is a reflection of the non-hyperbolicity of the method. The characteristic speeds ($\pm\sqrt{3/5}$) of P_3QS can be obtained from the Jacobian of Eq. (22) - (24) and these speeds are identical to the non-zero characteristic speeds of P_2 theory. They are different from the characteristic speeds ($\pm\sqrt{1/3}$) of P_1. But in figure 1 we see two peaks in the P_3QS solution moving at the characteristic P_1 speeds. To understand this, note that the wave speed of P_3QS looks like that of P_1 when the derivative of ψ_2^0 becomes 0. In the P_3QS solution ψ_2^0 should have a maximum at the location of the uncollided flux peaks, and examining the plot of ψ_2^0 in figure 2 we can see that this maximum coincides with the peaks moving at speeds $\pm\sqrt{1/3}$. Further, ψ_2^0 becomes smaller as time goes on, as shown in figure 2, and so the P_3QS solution behaves increasingly like the P_1 solution.

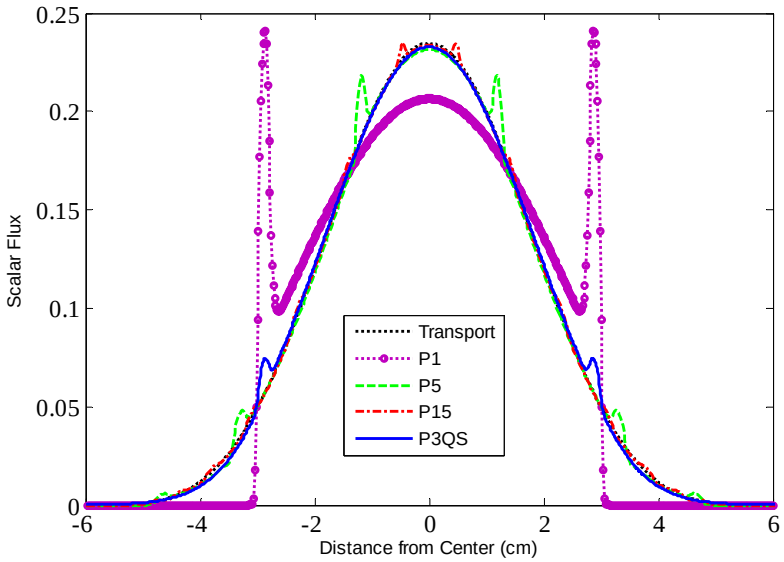

Figure 3. Comparison of P_3QS solution with P_1, P_5, P_{15} and transport solution at 5 seconds after the pulse

Figure 3 shows a comparison of P_3QS, P_1, P_5, P_{15} and the transport solution at 5 seconds after the pulse. P_3QS is closer to the transport solution than either P_1 or P_5 and it looks close to the P_{15} results. But P_3QS is much more efficient than P_{15} because it has fewer unknowns and requires fewer computational resources. P_{15} has 16 unknowns per cell, but P_3QS has only 4 unknowns.

5.2. Two-dimensional problem

Our two-dimensional test problem is a 4-cm square purely scattering medium ($\Sigma_t = \Sigma_s = 1$ cm^{-1}). A pulsed line source is imposed as an initial condition at the center of the system and vacuum boundary conditions are used.

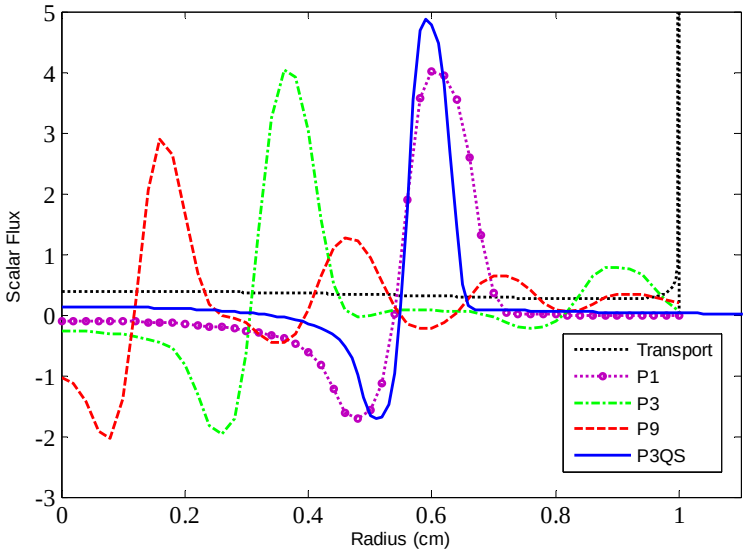

Figure 4. Comparison of P_3QS with P_1, P_3, P_9 and the transport solution at 1 second after the pulse

Figure 4 shows a comparison of the P_3QS solution with P_1, P_3, P_9 and the transport solution at one second after the pulse. From this figure we see that none of the P_N results is a good approximation to the transport solution because the scalar fluxes become negative. Also, the higher order P_N methods are increasingly oscillatory. But we can see that P_3QS is less negative and less oscillatory than any of the P_N results. Also it shows a positive flux near the center of the domain, although it still has a negative dip behind the front of uncollided particles.

Figure 5 shows a comparison of the solutions at 5 seconds after the pulse. At this time, all of the P_N solutions have become positive but they still have oscillations, although the higher order solutions are less oscillatory and closer to the transport solution. But P_3QS is less oscillatory and closer to the transport solution than any other P_N results. P_9 looks close to P_3QS but it has far more unknowns per cell than P_3QS (55 vs. 6).

Figure 6 shows the negative fluxes for P_3QS and P_1 solutions computed using a high-resolution Riemann solver with 50 and 100 cells/cm at 0.5 second after the pulse. This shows that P_3QS is less negative than the P_1 solution, but the negative spike behind the wave is better resolved as the spatial resolution increased.

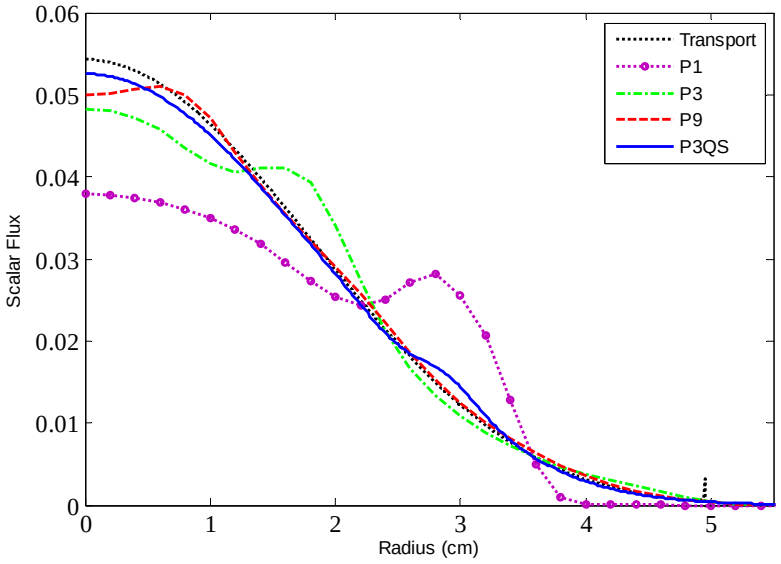

Figure 5. Comparison of P_3QS solution with P_1, P_3, P_9 and transport solution at 5 seconds after the pulse

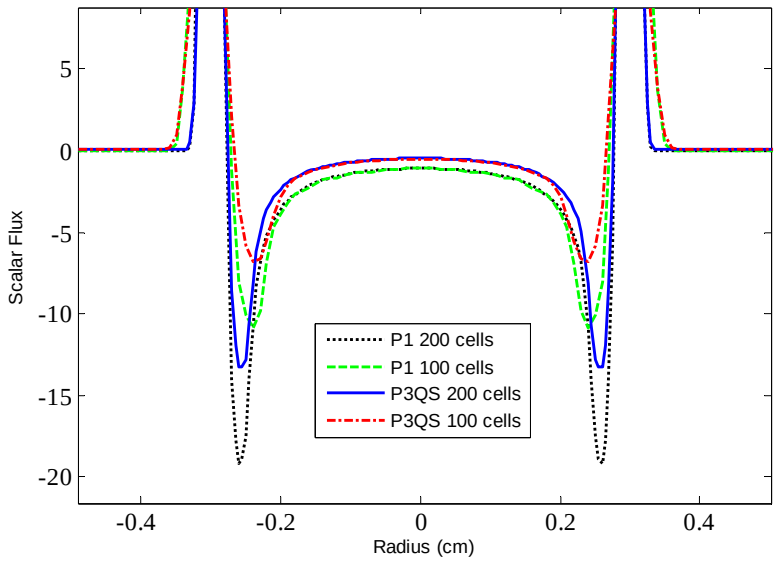

Figure 6. The negative fluxes for P_3QS and P_1 solutions at 0.5 second after the pulse

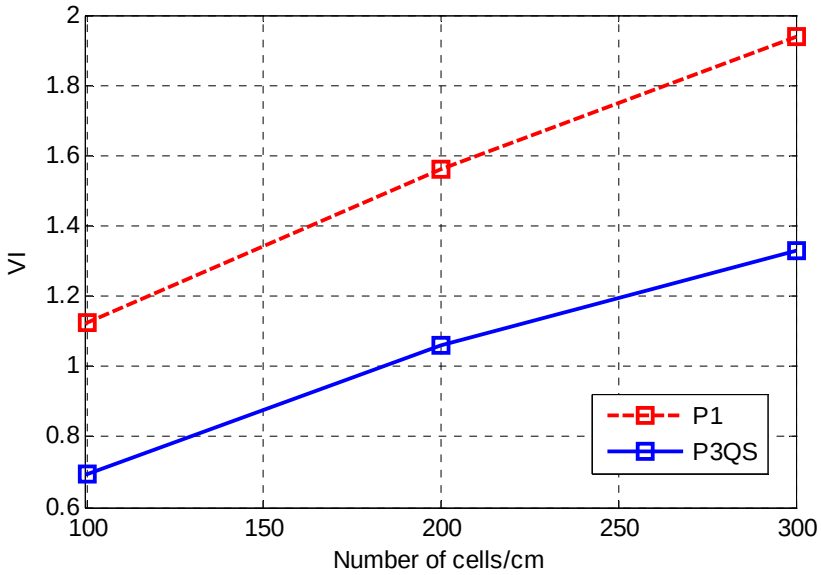

Figure 7. Comparison of the volume integrals of negative fluxes for P_3QS and P_1

In order to see the convergence of the negative flux in the negative region the volume integral of scalar flux is defined as,

$$\mathbf{VI} = \int_{-2}^{2}\int_{-2}^{2}\left(\left|\psi_0^0\right| - \psi_0^0\right) dz\, dx \tag{27}$$

where ψ_0^0 is a scalar flux. Fig. 7 shows a comparison of this volume integral for P_3QS and P_1 solutions as a function of the number of cells at 0.5 second. As the number of cells increases, **VI** for both solutions increases. Note however that **VI** for the P_3QS method is always smaller than that for the P_1 method.

5.3. Varying scattering ratio

So far all our results have been for a pure scatterer. Here we briefly present some results for various scattering ratios. Figure 8 and figure 9 show the solutions for the various scattering ratios $\left(c = \Sigma_s / \Sigma_t\right)$ at 1 second in 1D and 2D respectively. Here, the plot of $c = 0$ implies the solution in pure absorber and $c = 1$, pure scatterer. From these figures we can see that the collided fluxes shown between the wave fronts increase fast as the scattering ratio increases.

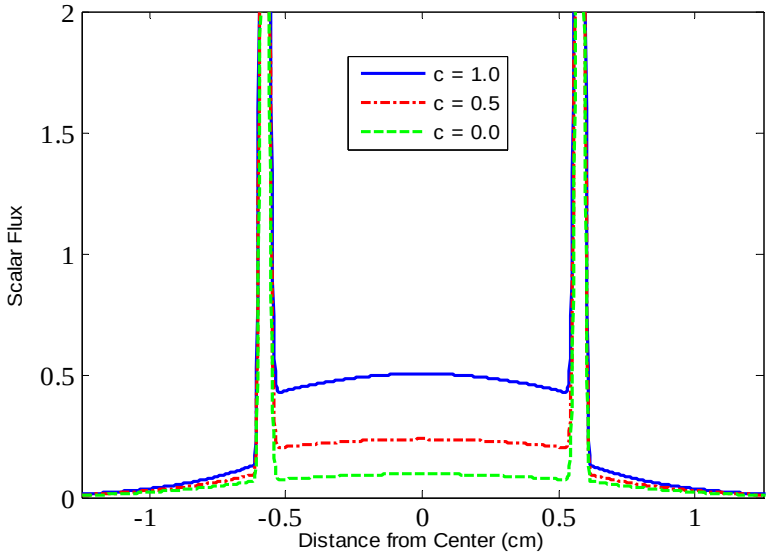

Figure 8. P_3QS **solution for various scattering ratios at one second in 1-D**

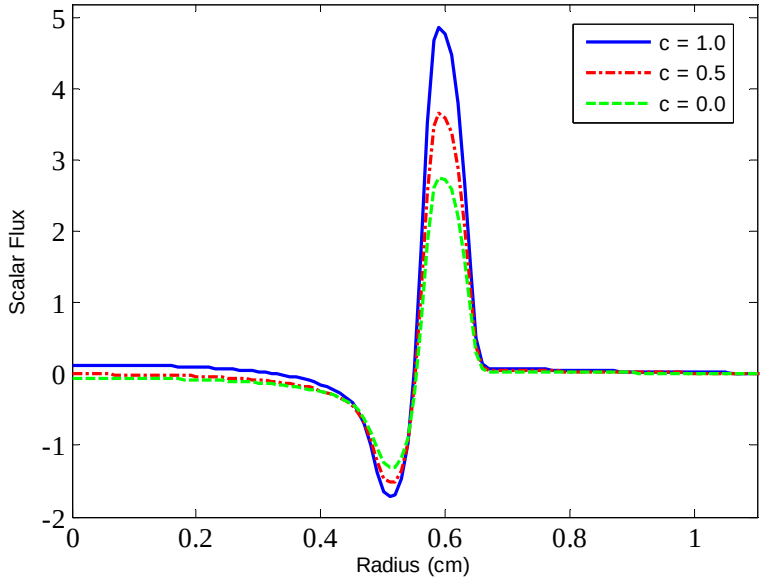

Figure 9. P_3QS **solution for various scattering ratios at one second in 2-D**

6. CONCLUSIONS

P_3 with a quasi-static closure (P_3QS) was suggested and has now been implemented. It is somewhat superior to other P_N closures because it has fewer unknowns for a given angular order, and produces a less negative scalar flux at the early times. Somewhat surprisingly, P_3QS is usually more accurate than P_3 and more accurate than higher order P_N methods. However, it does still produce negative scalar fluxes during a rapid transient (less than about one collision time). Further, like the diffusion theory, P_3QS is not useful in a vacuum because the equations become singular as Σ_t goes to 0. A truly robust, practical, time-dependent spherical harmonic closure with higher angular orders still eludes us.

ACKNOWLEDGMENTS

This work was supported in part by the DOE NNSA under the Predictive Science Academic Alliances Program by grant DE-FC52-08NA28616.

REFERENCES

1. T.A. Brunner, J.P. Holloway, “Two-dimensional time dependent Riemann solver for neutron transport,” Journal of Computational Physics, **Vol. 210**, pp.386-399 (2005).
6. R.G. McClarren, “Spherical Harmonics Methods for Thermal Radiation Transport,” Ph.D. Thesis, University of Michigan, Ann Arbor, Michigan, (2007).
3. R.G. McClarren, J. P. Holloway, T. A. Brunner, T. A. Mehlhorn, “A quasi-linear implicit Riemann solver for the time-dependent P_N equations,” Nuclear Science and Engineering, **Vol. 155**, pp.290-299 (2007).
4. R.G. McClarren, J. P. Holloway, T. A. Brunner, “On Solutions to the P_N equations for thermal radiative transfer,” Journal of Computational Physics, **Vol. 227**, (2008).
5. Minerbo, “Maximum Entropy Eddington Factors,” Journal of Quantitative Spectroscopy and Radiative Transfer, **Vol. 20**, pp.541-545 (1978).
6. J.E. Morel, T.A. Wareing, R.B.Lowrie, D.K. Parsons, Analysis of ray-effect mitigation techniques, Nucl. Sci. and Eng. 144, pp.1-22 (2003).
7. Martin Frank, Edward W. Larsen, “Time-dependent simplified P_N approximation to the equations of radiative transfer” Journal of Computational Physics, **Vol. 226**, pp.386-399 (2005)
8. Lewis, E.E and W. F. Miller, Jr., Computational Methods of Neutron Transport, John Wiley &Sons, (1994).
9. B. van Leer, “Towards the ultimate conservative difference scheme. V. A second-order sequel to Godunov’s method,” Journal of Computational Physics, **Vol. 135**, pp.229-248 (1997).
10. B.D. Ganapol, “Solution of the one-group time-dependent neutron transport equation in and infinite medium by polynomial reconstruction,” Nuclear Science and Engineering, **Vol. 92**, pp.272-279 (1986).
11. B.D. Ganapol, “Homogeneous infinite media time-dependent analytic benchmarks for X-TM transport methods development,” Los Alamos National Laboratory, March, (1999).